Contents of this file

Text S1

Figures S1-S12

Introduction

This supporting information contains:

- an extended description of the approaches used, respectively, to integrate simulations with expert elicitation outcomes and to obtain probabilistic hazard maps and curves (Text S1);
- the maps for fixed water depth for thresholds 0.1, 0.2 and 1 m for the Databases A and B and for volumes 1-30 × 10^6 m^3 and ≥ 1 × 10^6 m^3 (Figures S1-S6);
- the maps for fixed probability 2% for the Databases A and B and for volumes 1-30 × 10^6 m^3 and ≥ 1 × 10^6 m^3 (Figures S7-S8);
- the hazard curves for the 6 sites listed in Figure 1 from the main manuscript for the Databases A and B and for volumes 1-30 × 10^6 m^3 and ≥ 1 × 10^6 m^3 (Figures S9-S12).

Text S1

Integration of simulations with expert elicitation outcomes

To derive the hazard maps, we used the outputs of the CM method (see Section 2.1 of the main manuscript) and adopt the following procedure to derive probabilities for each specific volume/position interval. The ELICIPY tool (de' Michieli Vitturi et al., 2024), used for the elicitation described in Tadini et al. (submitted), generates a set of 10,000 probability values for each target question, representing the aggregated expert judgment. For this study, we thus obtained a set of 10,000 values for each of the target questions TQ16–TQ35. These questions are structured in a logic tree (see Figure. Level 1 questions (TQ16–TQ19) concern the marginal probabilities of a landslide's center of mass falling into one of four elevation ranges. Level 2 questions (TQ20–TQ35) provide the conditional probabilities for different volume classes, given a specific elevation range. To derive the absolute probabilities for each mutually exclusive volume/position interval, we performed the following calculation for each of the 10,000 sampling steps: the sampled probability value from a level-2 question (e.g., TQ20, the probability of a volume in class V1, given a deep submarine position) was multiplied by the corresponding sampled value from the relevant level-1 question (TQ16, the probability of a deep submarine position).

This calculation was performed for both of our analysis approaches. For the 1-30 × 10^6 m^3 case, this process considered the 3 bounded volume classes, yielding a matrix of 10,000 rows and 12 columns (4 position ranges × 3 volume classes). For the ≥ 1 × 10^6 m^3 case, which includes the V4 volume class, the same procedure was applied to all 4 volume classes, resulting in a matrix of 10,000 rows and 16 columns (4 position ranges × 4 volume classes). In both cases, each row of the resulting matrix represents a complete, internally consistent set of probabilities for the respective intervals. The values in each row were then normalized to sum to 1 to account for any minor inconsistencies arising from the sampling process. The final output consists of these two matrices of absolute probabilities (10,000x12 and 10,000x16), which are then used to assign probabilities to the simulated scenarios.

As stated above, the main challenge in assigning these probabilities lies in bridging the gap between the elicited interval-based probabilities and the discrete nature of the simulation database. To address this, we developed a sampling procedure to apportion the probabilities from the two matrices (10,000x12 and 10,000x16 matrices) across the relevant discrete simulations. This procedure is based on the key assumption that the probability for an elicitation interval is uniformly distributed within its parameter space. The procedure is executed independently for each of the 10,000 probability sets (i.e., for each row of the matrices) and consists of the following steps:

1. Generate Random Scenarios within each Interval. For each probability interval (12 for the 1-30 × 10^6 m^3 case; 16 for the ≥ 1 × 10^6 m^3 case), we generate 20 random scenarios by sampling uniformly from its defined volume and elevation ranges. The density contrast for each of these randomly generated scenarios is also selected from a uniform distribution between 0.5 and 0.6. This process creates a total of 240 (for the 1-30 × 10^6 m^3 case) or 320 (for the ≥ 1 × 10^6 m^3 case) hypothetical, intermediate scenarios.
2. Map to Closest Simulated Scenarios. Each of these hypothetical scenarios is then mapped to the closest available simulation in the corresponding database subset (Figure 3 from the main document visually illustrates this mapping process for the volume range 1-30 × 10^6 m^3). This step identifies a set of 240 (or 320) - not necessarily distinct— simulations that are considered representative of the continuous probability distributions within the intervals.
3. Partition and Aggregate Probabilities. The probability of each interval is divided equally among its 20 corresponding representative simulations. The final probability for each discrete simulation is then calculated as

the sum of all the probability portions it has received from the various intervals. Simulations that are never selected as the "closest" receive a final probability of zero for that sampling step.

This approach, by sampling each interval multiple times, effectively smooths the probability distribution across the discrete simulation set, providing a more robust representation of uncertainty than assigning an entire interval's probability to a single scenario.

The exceedance probabilities derived so far are conditional on the occurrence of a single tsunamigenic landslide within the Sciara del Fuoco. To convert these into absolute probabilities over a 50-year time horizon, we account for the expected frequency of events by incorporating the 10,000 sampled values from elicitation questions TQ3 (number of events in 50 years, N_{50}) and TQ4 (percentage within the Sciara del Fuoco - SdF, P_{SdF}). For each of the 10,000 sampling steps, we calculate a 50-year exceedance probability at every pixel. Since the expected number of events ($n = N_{50} \times P_{SdF}$) is a real number, we discretize its effect by considering the two closest integers, N_{low} and N_{up}. The conditional exceedance probability of a single event (p) is first used to compute the probability of at least one exceedance assuming N_{low} events and N_{up} events [$P(k) = 1 - (1 - p)^k$]. The final 50-year exceedance probability is then calculated as a weighted average of these two outcomes, where the weights are determined by the proximity of the sampled real number n to its integer neighbors. This entire procedure is repeated for all 10,000 sampling realizations, yielding a full distribution of 10,000 values for the 50-year exceedance probability at each pixel. This distribution fully captures the propagated uncertainty from both the source parameters and the event frequency. The final probabilistic maps were produced for water depth exceedance thresholds of 0.1, 0.2, 0.5, and 1 m. For each threshold, we present three maps corresponding to the 5th, Median, and 95th percentiles of the 10,000 fifty-year exceedance probability values calculated for each pixel.

The final output of this procedure consists of two distinct sets of probability vectors. For the 1-30 $\times$ 10^6 m^3 analysis, we obtained a set of 10,000 vectors, each containing 286 probability values corresponding to the simulations with volumes up to 30 $\times$ 10^6 m^3. For the $\geq$ 1 $\times$ 10^6 m^3 analysis, which includes the 40 $\times$ 10^6 m^3 scenarios, we obtain a separate set of 10,000 vectors, each containing 308 probability values. In both cases, each vector represents a complete probability distribution across the relevant set of discrete scenarios and serves as the foundational input for deriving the probabilistic inundation maps and hazard curves.

To generate the probabilistic maps for a fixed water depth threshold, we follow a procedure in line with standard Probabilistic Tsunami Hazard Assessment (PTHA) methodologies (e.g., Grezio et al., 2017; Selva et al., 2021). The process consists of the following steps:

- Set a Threshold and Binarize Maps. A specific water depth threshold is chosen (e.g., 0.5 m). Each of the 286/308 deterministic inundation maps is then converted into a binary map, where a pixel has a value of 1 if its water depth exceeds the threshold, and 0 otherwise.
- Calculate Exceedance Probability for a Single Realization. For each row of the probability matrix (representing one complete "realization" of the source uncertainty), we calculate a corresponding map of exceedance probabilities. For a given pixel, this is done by summing the products of the binary map values (0 or 1) and their corresponding probabilities from that row. The result for each pixel is the total probability of exceeding the threshold for that single realization.
- Generate the Full Distribution of Exceedance Probabilities. This process is repeated for all 10,000 rows of the matrix. Consequently, for every pixel in the domain, we obtain a distribution of 10,000 exceedance probability

values. This distribution fully captures the uncertainty in the exceedance probability, as derived from the expert elicitation.

From this distribution of 10,000 values at each pixel, we can then compute summary statistics, such as the 5th, 50th (median), and 95th percentiles. These percentile values are finally used to create the probabilistic inundation maps for the chosen threshold.

Development of Probabilistic hazard maps and curves

The process to obtain probabilistic hazard maps for a given water depth threshold consists of the following steps:

- set a threshold (e.g., 0.5 m) and binarize each of the 286/308 maps (pixel value 1 if its water depth exceeds the threshold, and 0 otherwise);
- calculate exceedance probability for a given pixel by summing the products of the binary map values (0 or 1) and their corresponding probabilities from that row;
- generate the full distribution of exceedance probabilities, obtaining a distribution of 10,000 exceedance probability values. From this distribution of 10,000 values at each pixel, we can then compute summary statistics, such as the 5th, 50th (median), and 95th percentiles. These percentile values are finally used to create the probabilistic inundation maps for the chosen threshold.

The final probabilistic maps were produced for water depth exceedance thresholds of 0.1, 0.2, 0.5, and 1 m. For each threshold, we present three maps corresponding to the 5th, Median, and 95th percentiles of the 10,000 fifty-year exceedance probability values calculated for each pixel.

The second category of hazard maps visualizes the water depth corresponding to a given exceedance probability. These maps represent the uncertainty in the inundation intensity for a specific likelihood level, providing a complementary perspective to the probability exceedance maps. The generation of these maps is performed for every pixel of the domain. For each of the 10,000 sampling realizations (i.e., each row of the probability matrix), we first construct a discrete cumulative probability distribution of water depth by summing the probabilities of the sorted simulation outcomes at a given pixel. From this distribution, we then identify the water depth value that corresponds to the desired exceedance probability (e.g., 10%). Repeating this process for all 10,000 realizations yields a distribution of 10,000 water depth values for each pixel. Each value in this distribution represents a plausible inundation depth for the chosen exceedance probability, reflecting the uncertainty propagated from the expert elicitation. From this distribution of water depths, we then compute summary statistics, such as the 5th, 50th (median), and 95th percentiles. The final maps display these percentile values, thus illustrating the range of likely water depths for a given probability of exceedance. In this paper, we present maps for an exceedance probability of 10% and show the results for the 5th, Median, and 95th percentiles.

To better characterize the hazard for specific sites of interest, we derive hazard curves. These curves describe the probability of exceeding a range of water depth values at a given location and are a standard tool in probabilistic tsunami hazard assessment (e.g., Volpe et al., 2019). The procedure to obtain them is applied independently to both the 1-30 $\times$ 10^6 m3 and the $\geq$1 $\times$ 10^6 m^3 analysis cases and is as follows.

First, for each simulation in the relevant database subset (286 or 308 simulations, respectively), we extract the exact water depth at the coordinates of each point of interest. Since these points do not typically coincide with the grid nodes of the

simulation, we use bilinear interpolation from the deterministic inundation maps. This step yields, for each site, an array of water depth values, one per simulation.

Next, we define a dense array of water depth thresholds, logarithmically spaced from 0.01 m to 20 m. For each of the 10,000 sampling realizations (i.e., each row of the corresponding 10,000x286 or 10,000x308 probability matrix), we compute a full hazard curve. This is done by calculating the probability of exceeding each threshold. For a given threshold, this probability is the sum of the probabilities (from the specific row of the matrix) of all simulations whose interpolated water depth at that site exceeds the threshold.

By repeating this calculation for every threshold, we obtain 10,000 distinct hazard curves for each site of interest. This ensemble of curves represents the full uncertainty in the hazard, as propagated from the expert elicitation. From this distribution of 10,000 curves, we compute the final hazard curves by taking the Median, 5^{th}, and 95^{th} percentiles of the exceedance probabilities at each water depth threshold.

Finally, these single-event hazard curves are converted to represent the hazard over a 50-year time horizon. This is achieved using the same procedure described for the inundation maps, which accounts for the sampled number of events in 50 years to calculate the final 50-year exceedance probabilities.

Figure S1. Probabilistic maps for exceeding a water depth of 0.1 m over a 50-year horizon for the Database B. (a) Volume range 1-30 × 10^6 m^3; (b) volume range ≥ 1 × 10^6 m^3.

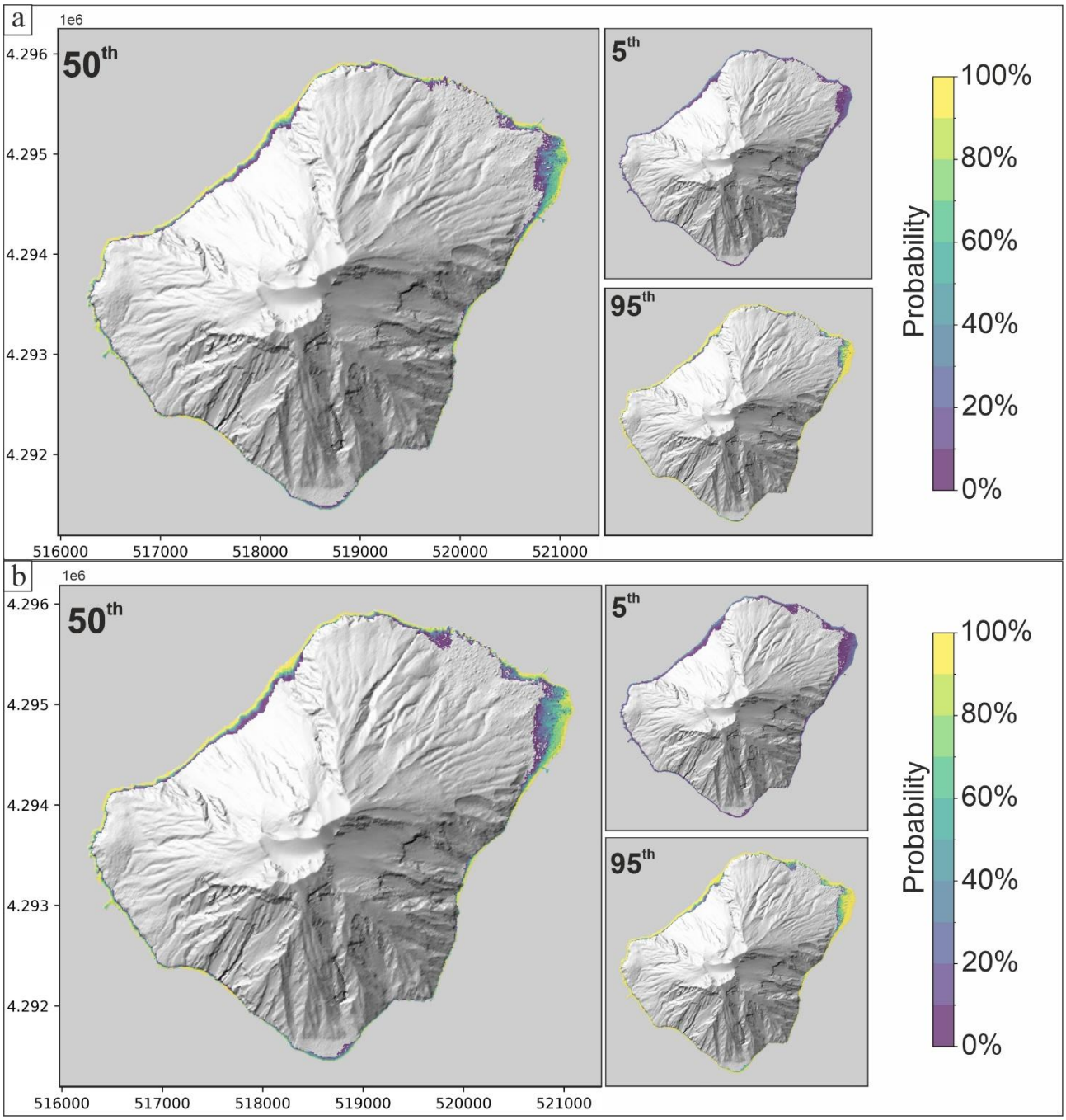

Figure S2. Probabilistic maps for exceeding a water depth of 0.1 m over a 50-year horizon for the Database A. (a) Volume range 1-30 × 10^6 m^3; (b) volume range ≥ 1 × 10^6 m^3.

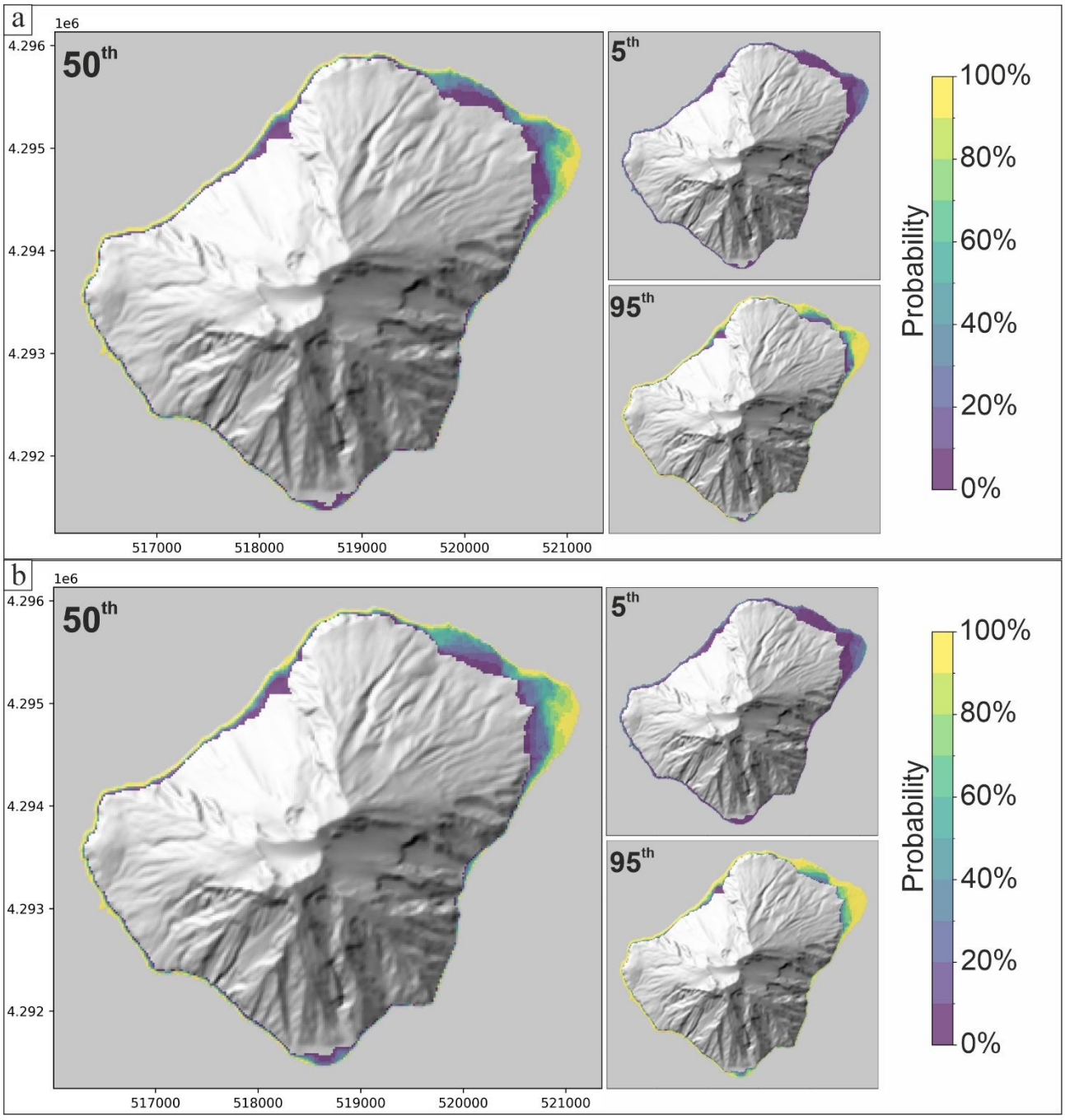

Figure S3. Probabilistic maps for exceeding a water depth of 0.2 m over a 50-year horizon for the Database B. (a) Volume range 1-30 × 10^6 m^3; (b) volume range ≥ 1 × 10^6 m^3.

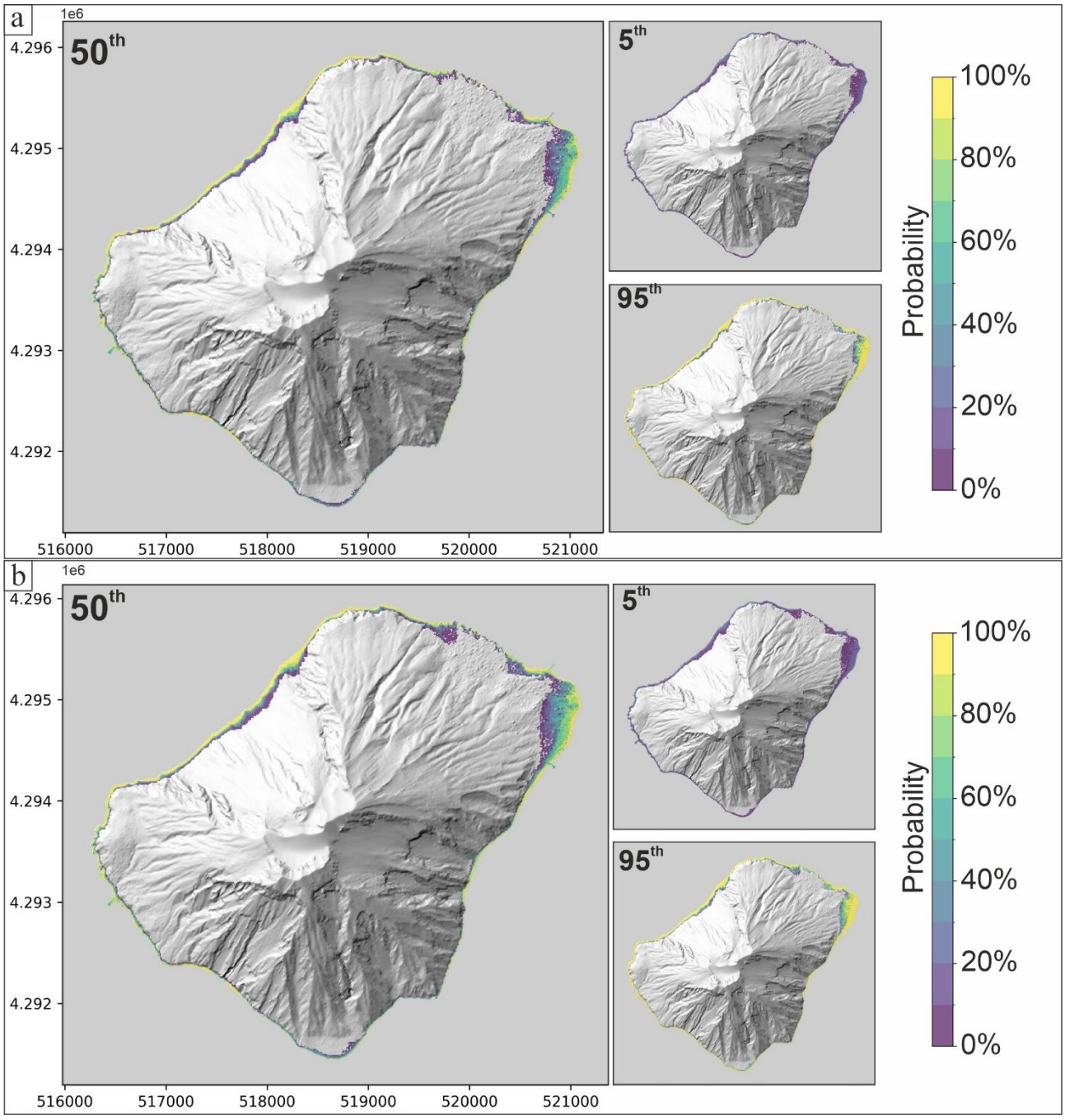

Figure S4. Probabilistic maps for exceeding a water depth of 0.2 m over a 50-year horizon for the Database A. (a) Volume range 1-30 × 10^6 m^3; (b) volume range ≥ 1 × 10^6 m^3.

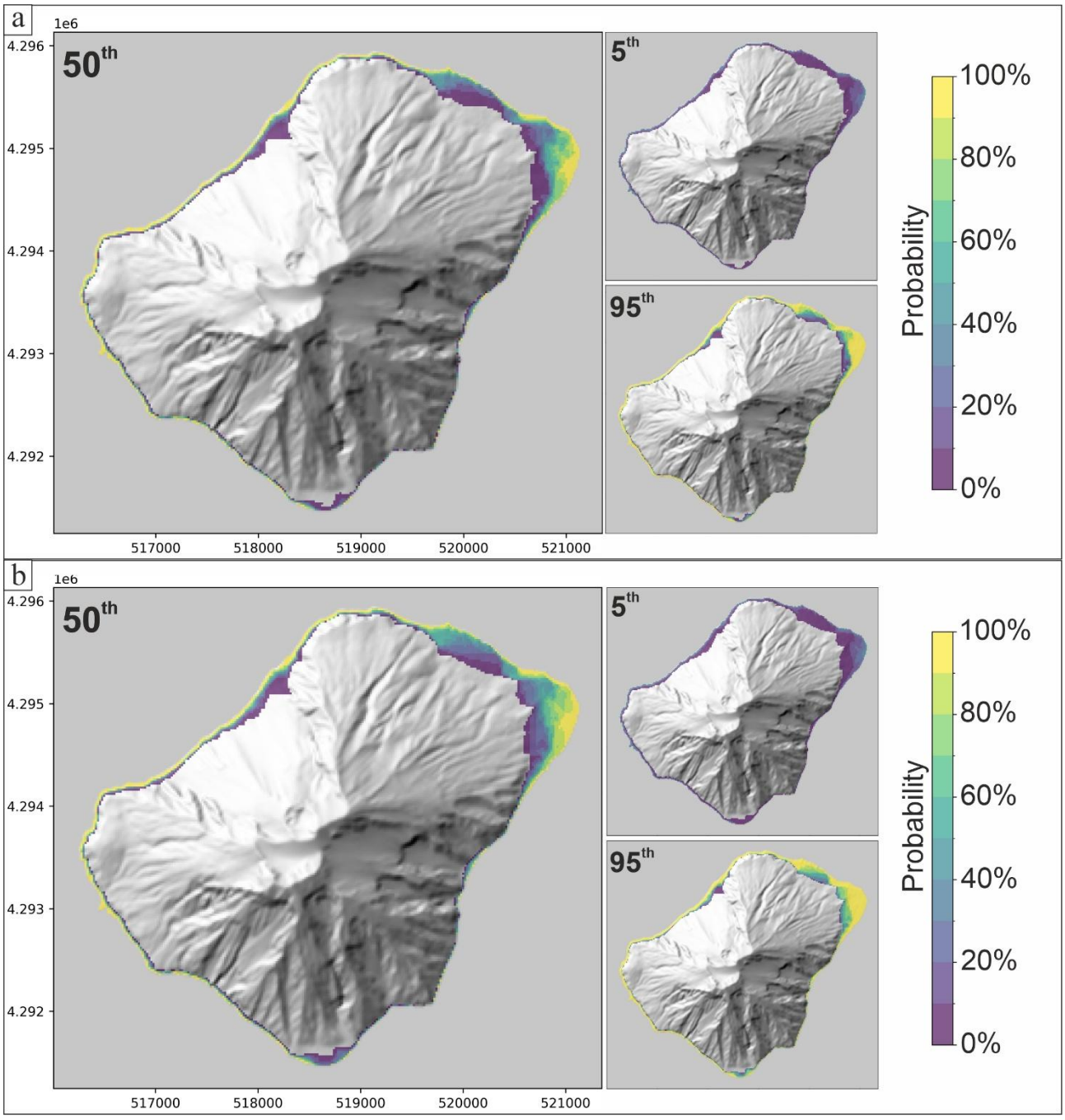

Figure S5. Probabilistic maps for exceeding a water depth of 1 m over a 50-year horizon for the Database B. (a) Volume range 1-30 × 10^6 m^3; (b) volume range ≥ 1 × 10^6 m^3.

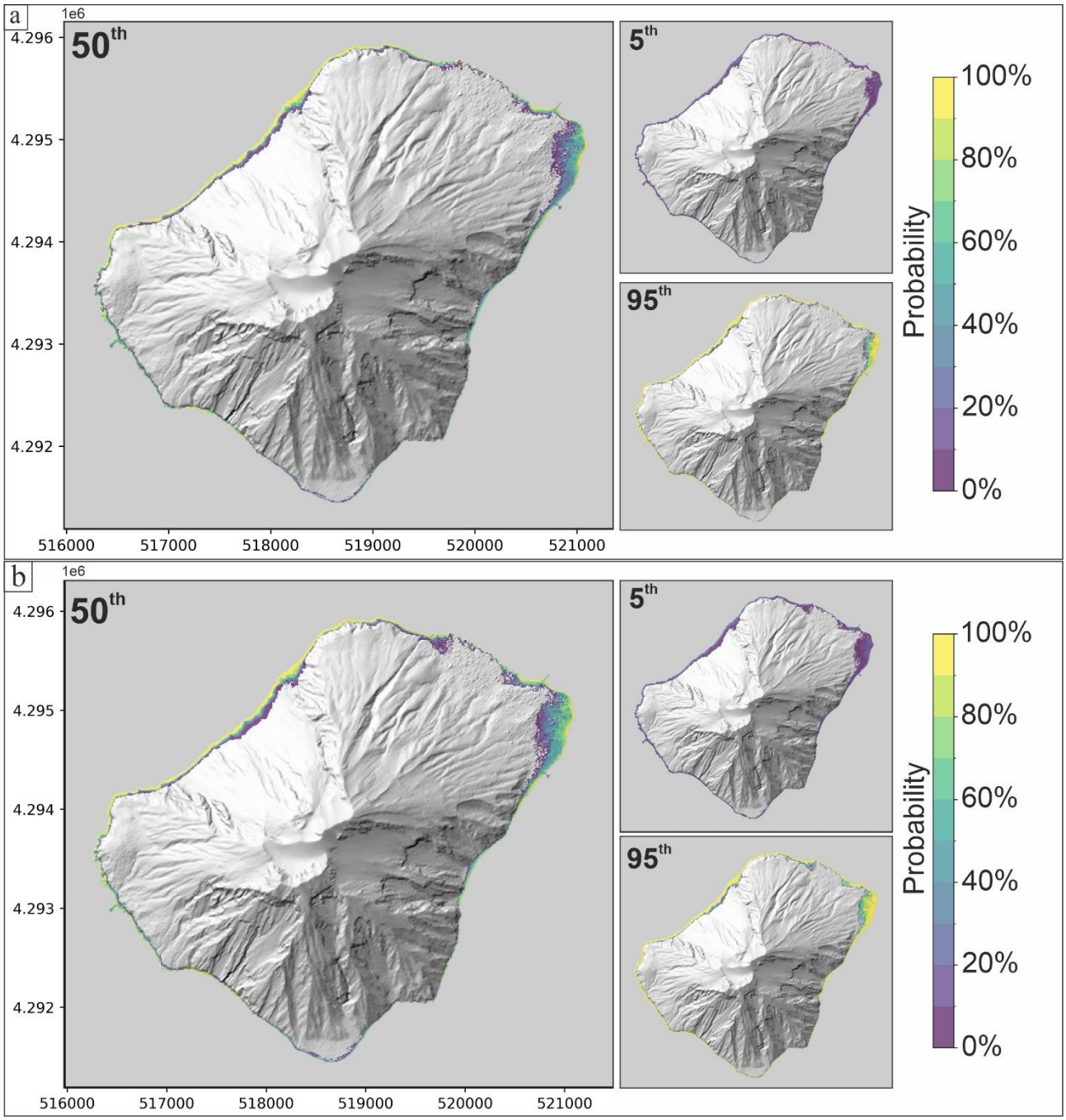

Figure S6. Probabilistic maps for exceeding a water depth of 1 m over a 50-year horizon for the Database A. (a) Volume range 1-30 × 10^6 m^3; (b) volume range ≥ 1 × 10^6 m^3.

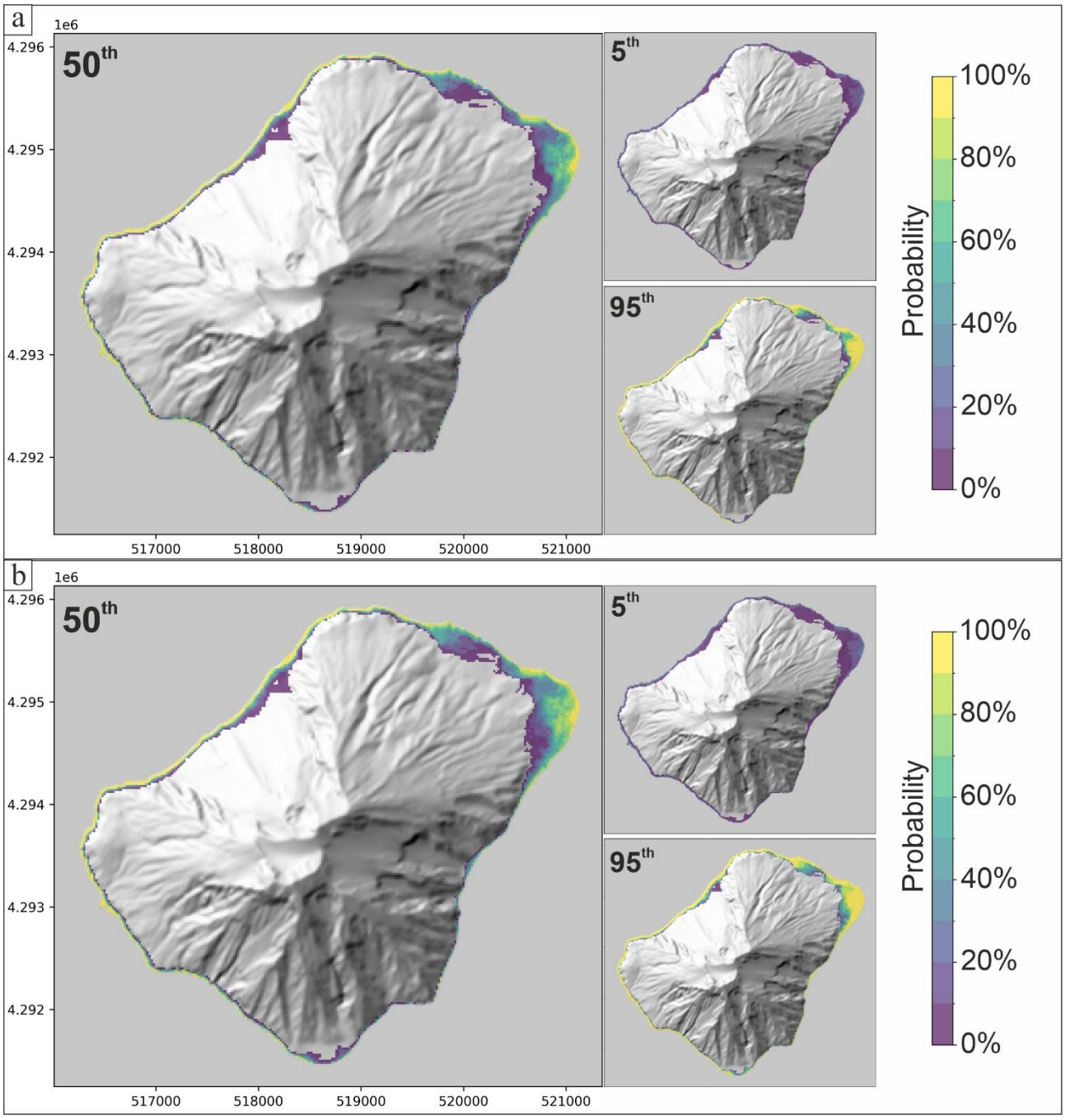

Figure S7. Probabilistic maps showing the inundation water depth corresponding to a 2% exceedance probability over a 50-year horizon for the Database B. (a) Volume range 1-30 × 10^6 m^3; (b) volume range ≥ 1 × 10^6 m^3.

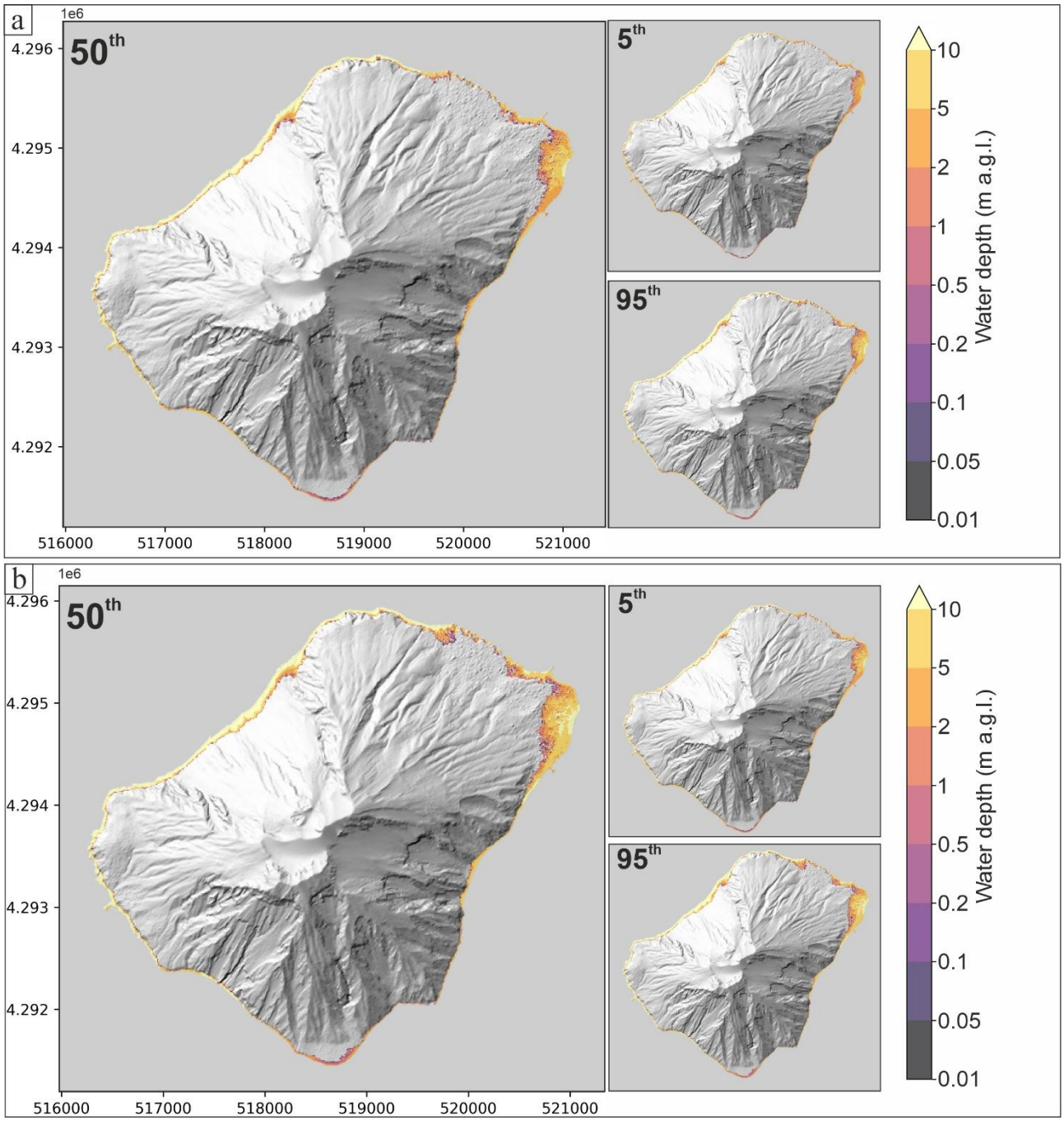

Figure S8. Probabilistic maps showing the inundation water depth corresponding to a 2% exceedance probability over a 50-year horizon for the Database A. (a) Volume range 1-30 × 10^6 m^3; (b) volume range ≥ 1 × 10^6 m^3.

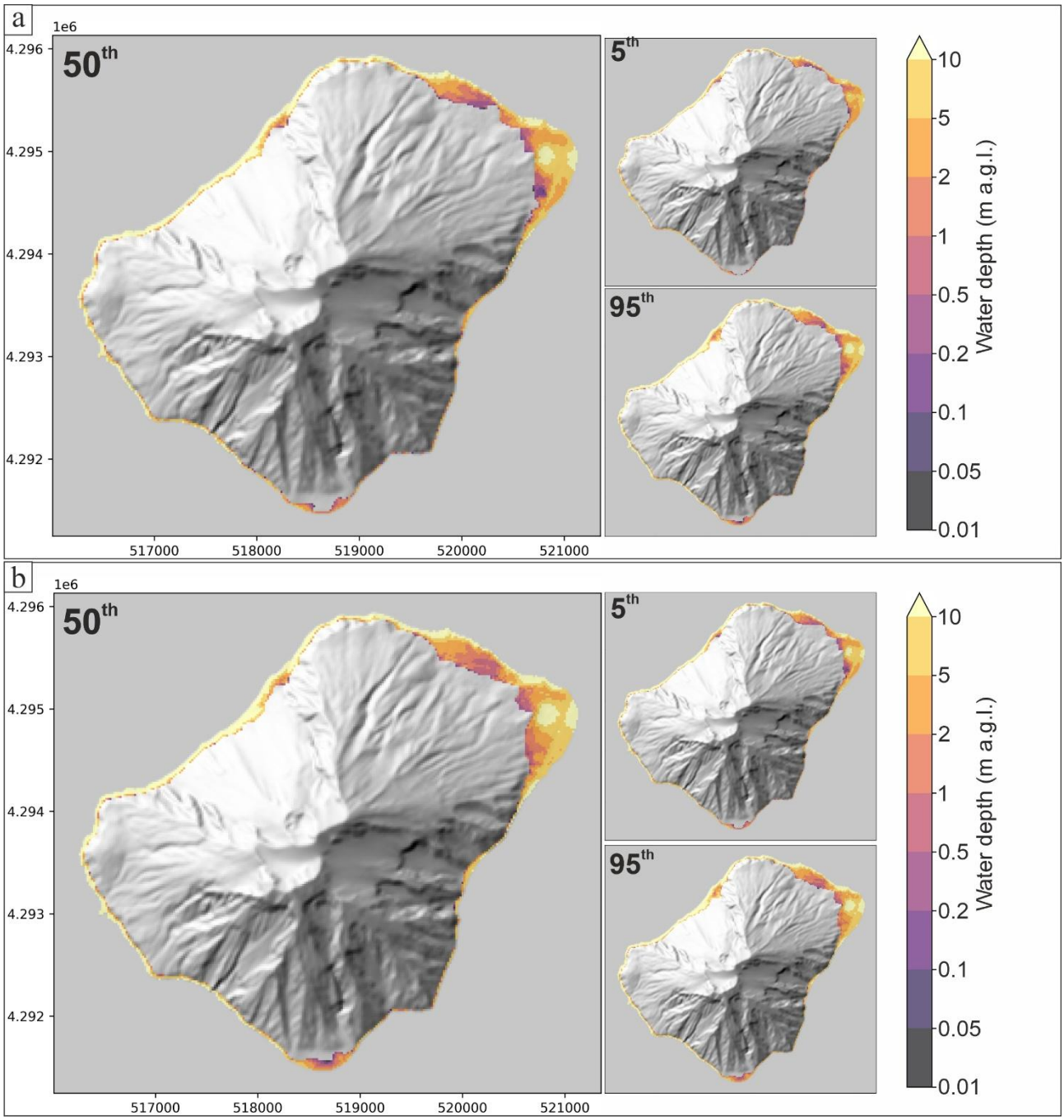

Figure S9. Probabilistic hazard curves for the 6 sites of Fig. 1 (main manuscript) for Database B, volumes 1-30 × 10^6 m^3. Each panel shows the 50-year exceedance probability as a function of water depth for the 5th, 50th, and 95th percentiles of the hazard distribution. Vertical grey dashed lines correspond to the water depth thresholds used for map production (0.1, 0.2, 0.5 and 1 m).

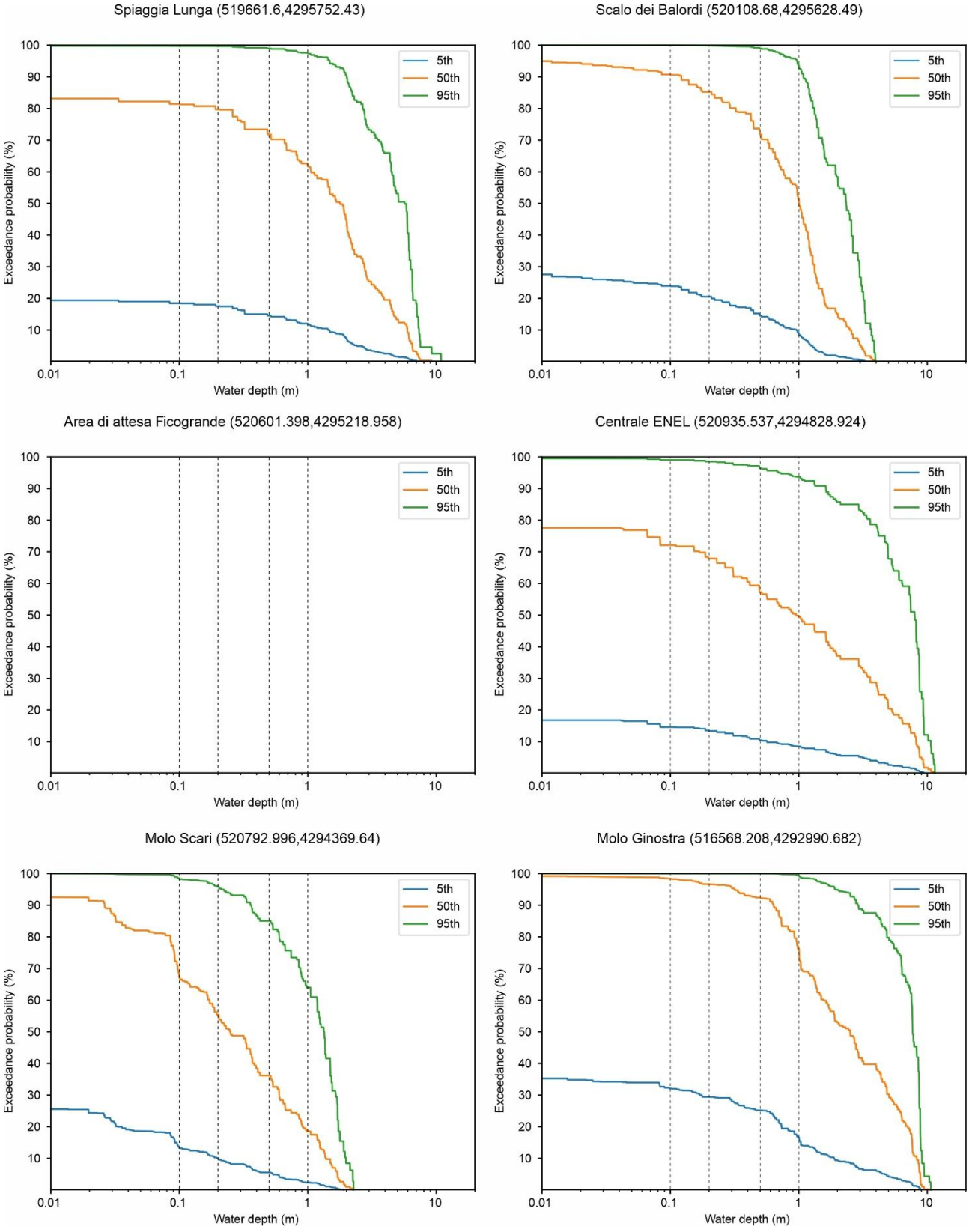

Figure S10. Hazard curves for the 6 sites of Fig. 1 (main manuscript) for Database B, volumes ≥ 1×10^6 m^3. Each panel shows the 50-year exceedance probability as a function of water depth for the 5th, 50th, and 95th percentiles of the hazard distribution. Vertical grey dashed lines correspond to the water depth thresholds used for map production (0.1, 0.2, 0.5 and 1 m).

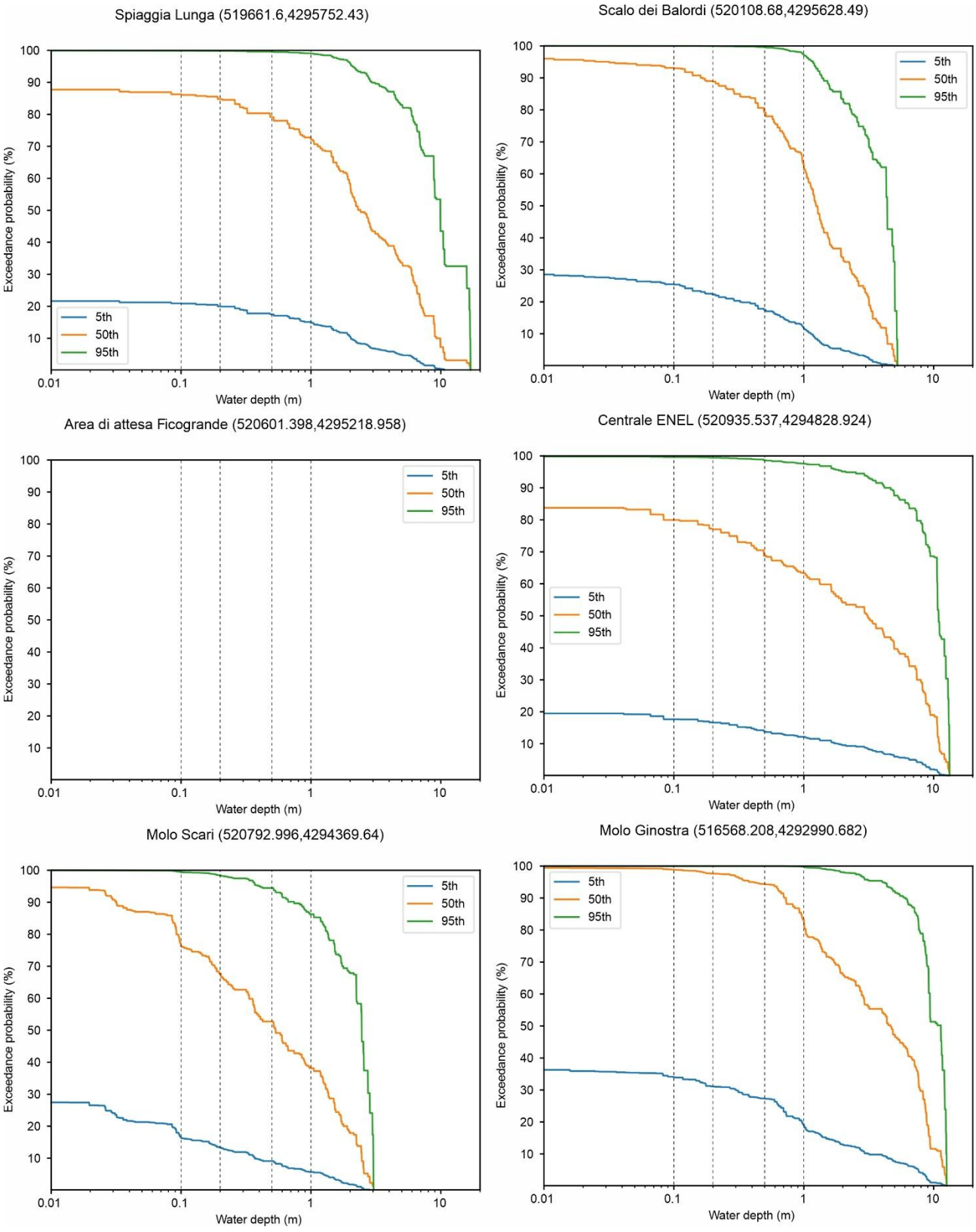

Figure S11. Hazard curves for the 6 sites of Fig. 1 (main manuscript) for Database A, volumes 1-30 × 10^6 m^3. Each panel shows the 50-year exceedance probability as a function of water depth for the 5^{th}, 50^{th}, and 95^{th} percentiles of the hazard distribution. Vertical grey dashed lines correspond to the water depth thresholds used for map production (0.1, 0.2, 0.5 and 1 m).

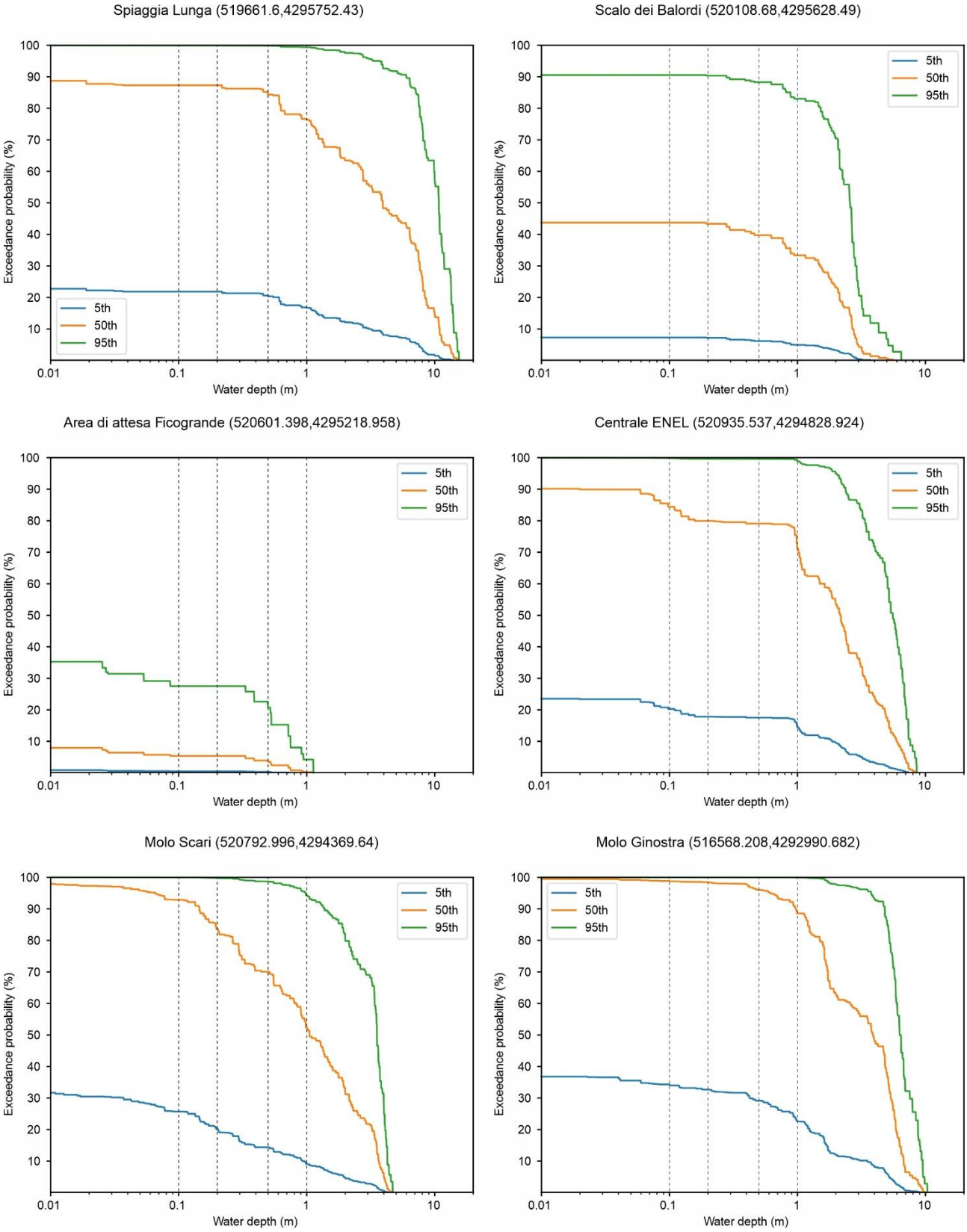

Figure S12. Hazard curves for the 6 sites of Fig. 1 (main manuscript) for Database A, volumes ≥ 1×10^6 m^3. Each panel shows the 50-year exceedance probability as a function of water depth for the 5th, 50th, and 95th percentiles of the hazard distribution. Vertical grey dashed lines correspond to the water depth thresholds used for map production (0.1, 0.2, 0.5 and 1 m).

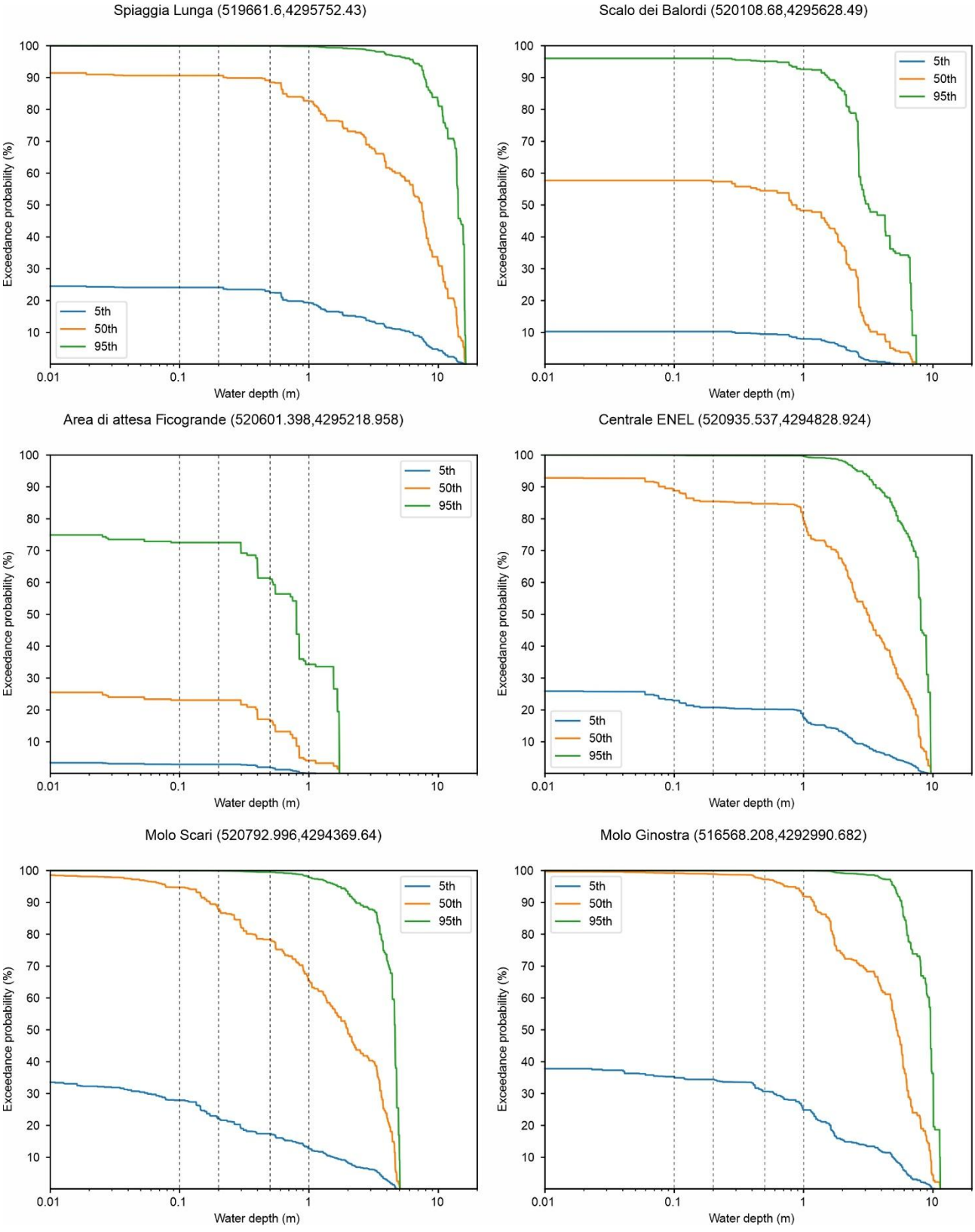

References

de' Michieli Vitturi, M., Bevilacqua, A., Tadini, A., Neri, A.: ELICIPY 1.0: a Python online tool for expert elicitation. SoftwareX, 25, 101641, doi: 10.1016/j.softx.2024.101641, 2024.

Grezio, A., Babeyko, A., Baptista, M. A., Behrens, J., Costa, A., Davies, G., Geist, E. L., Glimsdal, S., González, F. I., Griffin, J., Harbitz, C. B., LeVeque, R. J., Lorito, S., Løvholt, F., Omira, R., Mueller, C., Paris, R., Parsons, T., Polet, J., Power, W., Selva, J., Sørensen M. B., Thio, H. K.: Probabilistic tsunami hazard analysis: multiple sources and global applications. Reviews of Geophysics, 55(4), 1158-1198, doi: 10.1002/2017RG000579, 2017.

Selva, J., Lorito, S., Volpe, M., Romano, F., Tonini, R., Perfetti, P., Bernardi, F., Taroni, M., Scala, A., Babeyko, A., Løvholt, F., Gibbons, S. J., Macías, J., Castro, M. J., González-Vida, J. M., Sánchez-Linares, C., Bayraktar, H. B., Basili, R., Maesano, F. E., Tiberti, M. M., Mele, F., Piatanesi, A., Amato, A.: Probabilistic tsunami forecasting for early warning. Nature communications, 12(1), 5677, doi: 10.1038/s41467-021-25815-w, 2021.

Tadini, A., Bevilacqua, A., de' Michieli Vitturi, M., Bonilauri, E., Harris, A., Cerminara, M., Esposti Ongaro, T., Neri, A., Paris, R., Pistolesi, M., Trolese, M., Rodriguez Gàlvez, J. F., Andronico, D., Bertagnini, A., Calvari, S., Casalbore, D., Cassidy, M., Civico, R., Del Bello, E., Di Roberto, A., Fornaciai, A., Grezio, A., Gurioli, L., Harbitz, C. B., Lacanna, G., Løvholt, F., Marani, M., Pompilio, M., Rosi, M., Sandri, L., Urgeles, R., Voloschina, M.: Probabilistic tsunami hazard assessment at Stromboli volcano: 1. Review of historical sources and expert elicitation findings. Nat. Hazards Earth Syst. Sci., submitted.

Volpe, M., Lorito, S., Selva, J., Tonini, R., Romano, F., Brizuela, B.: From regional to local SPTHA: efficient computation of probabilistic tsunami inundation maps addressing near-field sources. Natural Hazards and Earth System Sciences, 19(3), 455-469, doi: 10.5194/nhess-19-455-2019, 2019.